Eur. Phys. J. B **30**, 343–349 (2002)
DOI: 10.1140/epjb/e2002-00388-1

THE EUROPEAN PHYSICAL JOURNAL B

# Study of $Ce(Rh_{1-x}Pd_x)_2Si_2$: pronounced differences between the $CeRh_2Si_2$ and $CePd_2Si_2$ ground states

M. Gómez Berisso[1,a], P. Pedrazzini[1], J.G. Sereni[1], O. Trovarelli[2], C. Geibel[2], and F. Steglich[2]

[1] Lab. Bajas Temperaturas, Centro Atómico Bariloche - IB (CNEA) and CONICET, 8400 S.C. de Bariloche, Argentina
[2] Max-Planck Institut for Chemical Physics of Solids, Nöthnitzer Str. 40, 01187 Dresden, Germany

Received 31 December 2001 / Received in final form 6 July 2002
Published online 19 December 2002 – 

**Abstract.** We present electrical resistivity and specific heat measurements of alloys on the Rh rich side of the phase diagram of the $Ce(Rh_{1-x}Pd_x)_2Si_2$ system. We compare these results with those obtained at intermediate and low Rh concentrations. The analysis of the concentration and temperature dependence of the entropy and of the scaling behaviour of $C_{el}(T)$ and $\rho(T)$ clearly confirm a separation of the magnetic phase diagram into two regions: the region $x \leq 0.3$, showing a concentration independent characteristic temperature for the $4f$-electrons with $T_0 \approx 45$ K, while for $x > 0.3$, $T_0$ decreases to $T_0(x = 1) \approx 15$ K. At low Pd-content, $T_N$ decreases very rapidly from $T_N = 36$ K in pure $CeRh_2Si_2$ to $T_N = 18$ K at $x = 0.1$. With higher Pd concentration $T_N$ stabilizes at $T_N \approx 15$ K whereas the magnitude of the anomalies in $C_{el}(T)$ and in the susceptibility around $T_N$ are further reduced and disappear at $x \approx 0.3$. This differs from the behavior found on the Pd-rich side, where $T_N$ decreases continuously to zero with increasing Rh content. The pronounced differences observed between both phase boundaries and the drastic effect of doping on the Rh rich side suggest an itinerant character in $CeRh_2$ $Si_2$, in contrast with the localized character of $CePd_2Si_2$. Further evidence for the itinerant character of $CeRh_2Si_2$ is given by the $\rho(T)$ dependence observed for $x \leq 0.3$, which scales with $\rho(T)$ of the prototype itinerant compound $YCo_2$.

**PACS.** 71.10.Hf Non-Fermi-liquid ground states, electron phase diagrams and phase transition in model systems – 71.27.+a Strongly correlated electron systems; heavy fermions

## 1 Introduction

The exceptionally high Néel temperature of $CeRh_2Si_2$, $T_N = 36$ K [1], remains a puzzling question after almost twenty years, because it has escaped the many attempts of explanation based on mechanisms applicable to other Ce intermetalic compounds. The exceptional magnitude of this $T_N$ can be appreciated by comparing it with that of $GdRh_2Si_2$ ($T_N = 90$ K) using the de Gennes factor [2], from which a difference of nearly two orders of magnitude is to be expected. The main difficulty for finding a realistic description of this compound is related to the fact that it lies within the as yet poorly defined boundary between the applicability of either *local* or *itinerant* models. In the local scenario, $f$-orbitals are not considered to be hybridized with ligand-orbitals, forming purely localized states. Magnetic exchange is then mediated by RKKY interaction. In the itinerant scenario, the hybridized $f$-ligand orbitals form extended states in the same way as $d$-electrons do. Magnetism is then described within spin-fluctuation and Stoner theory. In the case of $CeRh_2Si_2$, there are specific arguments in the literature supporting each type of model. For the localized moment scenario, one finds that: i) the ordered magnetic moment along the $c$-axis [3] ($m_o \cong 1.5\mu_B$ at $T = T_N/3$) is close to that of a Ce localized moment, after correcting for crystal electric field effects (CEF); ii) the previously reported specific heat jump [4] at $T = T_N$, $\Delta C_{el}(T_N) = 10$ J/molK, is close to the value for a local doublet system in a mean field theory; iii) in coincidence, the related entropy gain $\Delta S(T_N) \approx R \ln 2$ is close to the value expected for a doublet ground state (GS). Although a two step metamagnetic transition (observed at 26 tesla) was taken as evidence for a local moment system [5], this argument is not conclusive because metamagnetic transitions are also predicted for anisotropic itinerant systems [6], a strong anisotropy being a clear property of the system at hand [5]. Recent de Haas-van Alphen experiments were suggested as support for the local scenario at ambient pressure and for the itinerant scenario above the critical pressure where the antiferromagnetic order disappears [7]. However these results are not conclusive because the Fermi-surface experimentally observed at ambient pressure is much more complex than the calculated one, probably due to the effect of the magnetic order. Furthermore, as explicitly stated in

[a] e-mail: berisso@cab.cnea.gov.ar

reference [7], the calculated Fermi-surfaces are very similar for the localized and the itinerant scenarios.

A strong mixing between the Ce-4$f$ and conduction states supporting the itinerant description was recognized early-on from the large Curie-Weiss temperature [3]: $\theta_W = -70\,\mathrm{K}$, suggesting a Kondo temperature ($T_\mathrm{K}$) even larger than $T_\mathrm{N}$ for this compound, though the strong anisotropy was observed in magnetic susceptibility ($\chi$) and thermal expansion on single crystals [8] with $\theta_{W\|c} \approx -40\,\mathrm{K}$ (in the $c$ direction) and a value four times larger in the basal plane. On the other hand, $T_\mathrm{K} \approx 33\,\mathrm{K}$ was obtained from the width of the quasi-elastic line in inelastic neutron scattering [9], whereas NMR results suggest a much higher value of $T_\mathrm{K} \approx 100\,\mathrm{K}$ [10]. Recent neutron scattering experiments showed a single $q$ antiferromagnetic structure below $T_N = 36\,\mathrm{K}$ and a 4-$q$ structure below a second transition at 25 K. Under pressure, the value of the ordered moment was found to decrease proportional to $T_N$, indicating an itinerant character for the magnetism [11]. From the Si-NMR results a much smaller magnetic moment ($m_o = 0.22\mu_B$) is estimated which, together with the high $T_\mathrm{N}$ value, suggests an itinerant character for the $CeRh_2Si_2$ magnetic ground state. The large difference in $m_o$ determined in neutron diffraction and Si-NMR experiments was attributed to the different characteristic times of these measurements, suggesting a dynamic nature for the magnetic order. Above $T_\mathrm{N}$, the electrical resistivity ($\rho$) increases with a characteristic energy scale of $T_0 \approx 200\,\mathrm{K}$, larger than $T_\mathrm{N}$ but comparable to the expected CEF splitting [5]. These values, together with the $\rho(T)$ variation under pressure, support the argument that band spin fluctuations contribute significantly to the conduction electron scattering [12].

Within the scope of a Doniach-type description [13], $CeRh_2Si_2$ is a paradigmatic case. With the highest $T_\mathrm{N}$ value among the $CeT_2Si_2$ compounds it has to be placed at the top of the Doniach diagram [14]. Such a position is consistent with the $T_\mathrm{N}$ evolution of the $CeRh_2(Si,Ge)_2$ system [15], where the increase of the volume due to the substitution of Si by Ge leads to a decrease in the value of $T_\mathrm{N}$. This argument is complemented by the pressure dependence measurements on stoichiometric $CeRh_2Si_2$, which also show a decrease in $T_\mathrm{N}$ down to about 10 K at approximately 1 GPa and the disappearance of the related anomaly above that pressure [16]. However, when the comparison is performed with respect to other $CeT_2Si_2$ compounds it becomes contradictory in terms of the absolute $T_\mathrm{N}$ and $T_\mathrm{K}$ values, because for T=Rh the Kondo temperature is much larger than that for T=Pd or Cu, despite the fact that these compounds have a "less magnetic" behavior [14]. The pressure effect shows that, despite the high $T_\mathrm{N}$ value, the magnetic order breaks down at the lowest pressure value within this family of Ce-compounds. The extreme sensitivity of this magnetic interaction is also evident with respect to $GdRh_2Si_2$ (there 1GPa reduces $T_\mathrm{N}$ by only 10% [2]), or $CePd_2Si_2$ (which requires a pressure three times higher to suppress the magnetic order despite the fact that $T_\mathrm{N}$ is three times lower [17]).

At present, the large amount of information accumulated on $CeRh_2Si_2$ is not conclusive enough to elucidate whether this compound has to be considered as *local* or *itinerant* in its magnetic behavior. This ambiguity is mainly related to the fact that it is placed at the peculiar position where the energies associated with competing parameters, like $T_\mathrm{N}$ and $T_\mathrm{K}$, are comparable. New independent information can be provided by studying the evolution of this system when those parameters are continuously modified driving the compound to a more *local* scenario. This purpose can be achieved only by selective alloying, because pressure increases the itinerant character by increasing the hybridization. The chance to enhance the local character is provided by partial substitution of Rh with Pd in the $Ce(Rh_{1-x}Pd_x)_2Si_2$ system, which was recently shown to form continuously [18]. A preliminary investigation indicated a complex magnetic phase diagram [19]. Taking advantage of the fact that $CePd_2Si_2$ behaves as a localized magnet, a direct comparison of both ends of the $Ce(Rh,Pd)_2Si_2$-phase-diagram should give more information about the nature of the magnetic state of $CeRh_2Si_2$.

## 2 Experimental and results

For the present detailed study, further samples on the Rh rich region and some reference $La(Rh_{1-x}Pd_x)_2Si_2$ alloys were prepared following the same sample preparation procedure and experimental techniques described previously [18,19].

Due to its sensitivity to the nature of the electronic scattering, the electrical resistivity is one of the physical properties to be investigated when a distinction between a local and an itinerant electronic character is required. As reported in Figure 1, in this system the temperature dependence of the electrical resistivity, $\rho(T)$, shows quite different features for both concentration extremes. Due to microscopic cracks in the sample, the geometrical factor, and consequently the absolute resistivity values, cannot be determined unambiguously. Therefore the $\rho(T)$ values were normalized at 250 K to permit a better comparison. As already mentioned in reference [5], in stoichiometric $CeRh_2Si_2$, $\rho(T)$ increases continuously with a characteristic energy scale of approximately 100 K. This behavior persists up to 30% of Pd doping, but above that concentration another relative maximum develops at low temperature (at approx. 20 K, as seen in Fig. 1b). This maximum becomes more pronounced with increasing Pd-content. The main feature is that the temperature of both resistivity maxima practically do not change with concentration, while the relative strength of the electronic scattering changes significantly. On the Pd rich side, the double maximum typical for trivalent Ce intermetallics compounds with $T_\mathrm{K} \ll \Delta_\mathrm{CEF}$ (CEF-splitting) is observed (see Fig. 1b). The maximum at low temperature is attributed to the electronic scattering by the GS while the the maximum at higher temperature is attributed to the excited CEF level, both being enhanced by the Kondo effect [20].

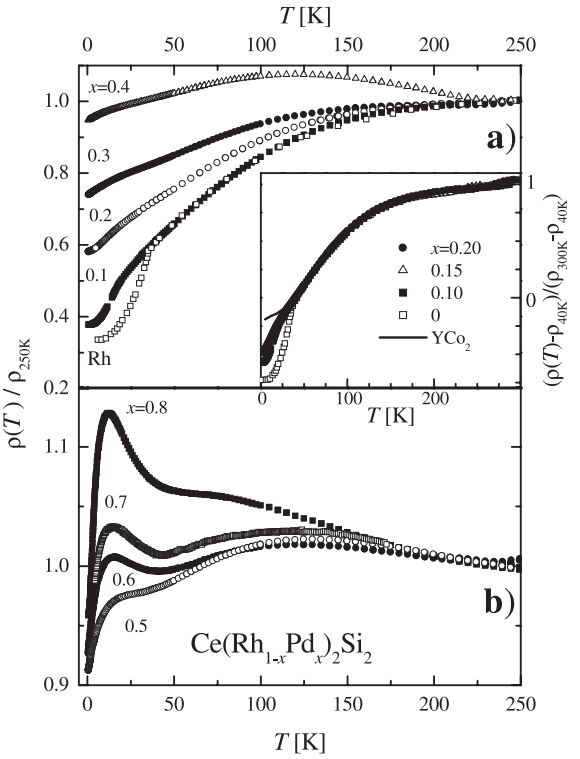


**Fig. 1.** Temperature dependence of the electrical resistivity normalized to their values at 250 K. a) Samples with $0 \leq x \leq 0.4$ and b) between $0.5 \leq x \leq 0.8$. Inset: scaling of the $\rho(T, x)$ dependence for the Rh-rich samples with $\rho(T)$ normalized at $T = 40$ K and 300 K. $\rho(T)$ of $YCo_2$ compound is also included for comparison. The data of the $x = 0$ sample was taken from reference [12].

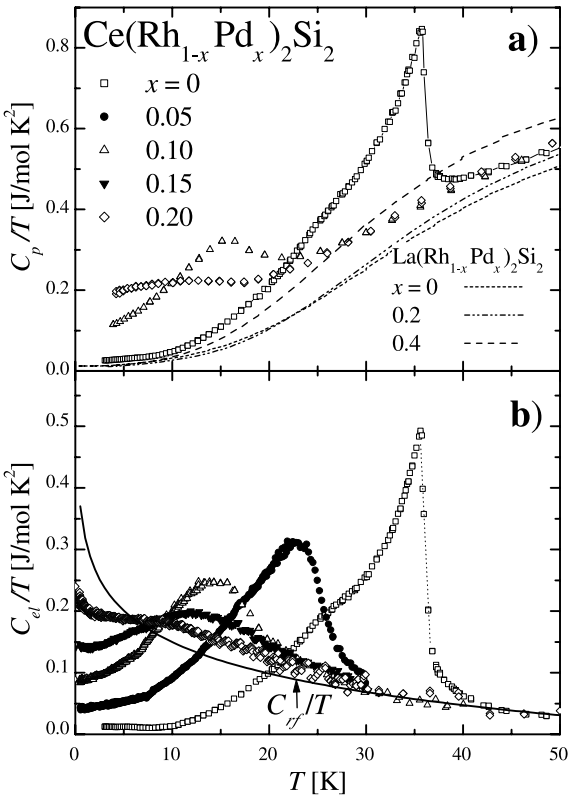


**Fig. 2.** a) Measured specific heat up to 50 K for some Rh-rich and (doted curves) some La–reference alloys. b) Electronic contribution to the specific heat of the Rh-rich samples ($0 \leq x \leq 0.2$). The solid curve ($C_{\rm rf}/T$) is the function taken as reference for the analysis of the entropy compensation (see text).

The temperature dependence of the electronic contribution to the specific heat ($C_{\rm el}/T$) at low Pd doping ($0 \leq x \leq 0.2$) is shown in Figure 2. This contribution was evaluated from the measured specific heat ($C_{\rm p}/T$) as: $C_{\rm el}/T = C_{\rm p}/T - C_{\rm ph}/T$, where $C_{\rm ph}/T$ is the phonon contribution extracted from La isotypic compounds with $x = 0$, 0.2, 0.4 and 1. As it can be seen in the upper part of Figure 2, the Ce-based samples on the Rh-rich side ($0 \leq x \leq 0.2$) show quite similar $C_{\rm p}/T$ values at $T \geq 40$ K, in coincidence with the isotypic La-based samples. In contrast, from $x \geq 0.4$ $C_{\rm ph}(T)/T$ increases with $x$ after a drastic enhancement between $x = 0.2$ and 0.4. This non-monotonous variation of $C_{\rm ph}$ upon Pd doping suggests a change in the phonon spectrum around $x = 0.3$.

Our sample of pure $CeRh_2Si_2$ shows a larger jump at $T_{\rm N}$, $\Delta C_{\rm el}(T_{\rm N}) = 15\,{\rm J/mol\,K^2}$, than previously reported in the literature [4], which exceeds the mean field prediction. This peak in $C_{\rm el}/T$ at $T_{\rm N}$ is better observed in thermal expansion [8], and is probably related to the opening of a magnetic excitation gap due to the strong Ising-type anisotropy of this compound. A further weak anomaly associated with the change of the magnetic propagation vector is also observed at 25 K [21]. A small amount of Pd ($x \leq 0.1$) leads to a strong decrease of $T_{\rm N}$ and a pronounced broadening of the anomaly in $C_{\rm el}(T)$. This broadening indicates that Pd doping in $CeRh_2Si_2$ destroy the coherence of the magnetic state quite strongly. Further increase of the Pd concentration ($0.1 \leq x \leq 0.4$) leaves the temperature of the maximum almost unchanged but reduces the size of the anomaly, which eventually disappears between $x = 0.3$ and $x = 0.4$. Due to the broadening, the analysis of the anomaly in $C_{\rm el}(T)$ does not lead to a reliable determination of $T_{\rm N}(x)$. More precise values can be obtained from the susceptibility by looking at the derivative $\mathrm{d}(\chi T)/\mathrm{d}T$ and defining $T_{\rm N}$ as the temperature of the maximum (see Fig. 3). This demonstrates very clearly the rapid drop of $T_{\rm N}$ from 36 K in pure $CeRh_2Si_2$ to 18 K at $x = 0.1$ and then the levelling off at around 15 K for $x \leq 0.2$ (see also the phase diagram in Fig. 7). This is in sharp contrast to the Pd-rich region, where $T_{\rm N}$ drops monotonously with increasing Rh content and extrapolates to 0 K at $x = 0.65$. The broadening of the anomaly is also much less pronounced on the Pd-rich side. The disappearance of the anomaly without a concomitant decrease of $T_{\rm N}$ to 0 K on the Rh-rich side indicates that the degrees of freedom involved in the magnetic transition as well as the free energy gained in that transition decrease with Pd content and eventually vanish, whereas $T_{\rm N}$ and thus the strength of the magnetic interaction still has a finite value.

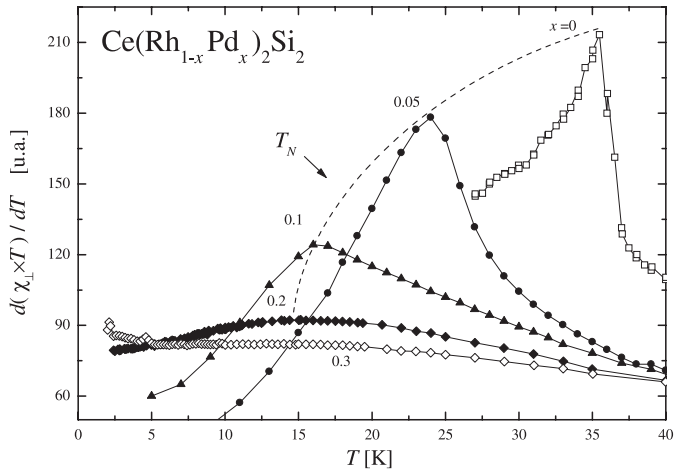


**Fig. 3.** Plot of the derivative of $\chi_\perp \times T$ as a function of temperature and concentration in order to better determine $T_{\rm N}(x)$ on the Rh-rich side. The magnetic response for field perpendicular to the textures was taken from reference [18].

The much stronger suppression of the magnetic order by Pd doping in $CeRh_2Si_2$ compared to the effect of Rh doping in $CePd_2Si_2$ is not due to a stronger lattice disorder on the Rh-rich side. This is evidenced by the composition dependence of the residual resistivity $\rho_0$, which was inferred from the composition dependence of the resistivity radio $RRR$, since a reliable determination of $\rho_0$ was prevented by the large amount of cracks in the alloy-samples. $\rho_0(\propto 1/RRR)$ increases more slowly with doping on the $CeRh_2Si_2$ side than on the $CePd_2Si_2$ side, showing a broad, asymmetric maximum between $x = 0.5$ and 0.8, this maximum being shifted towards the $CePd_2Si_2$ side.

Within the intermediate concentration region ($0.3 < x < 0.7$), $C_{\rm el}(T)/T$ is well described by a logarithmic decrease, with a downward curvature at low temperature, as typically observed in systems lying close to a magnetic instability [22]. The low temperature $C_{\rm el}/T$ value increases proportionally to the Pd-concentration up to $x = 0.7$, where the onset of the magnetic order of $CePd_2Si_2$ is observed.

## 3 Discussion

Since the intrinsic differences of the doping effect on $T_{\rm N}$ has been established between Pd and Rh rich sides, we shall analyze further properties to gain insight into the nature of the ground state on both extremes of the alloy system. The most important parameter is the characteristic energy related to the delocalization of the 4*f*-electrons. A rough idea about its dependence on the composition can be obtained by looking at the evolution of the entropy. In Figure 4a, we show the entropy gain as a function of temperature up to 50 K on the Rh-rich side, and in Figure 4b that of the intermediate and Pd-rich samples up to 14 K. Within the experimental dispersion, the entropy gains in the Rh-rich samples merge above the respective $T_{\rm N}(x)$ into a common curve. As it will be shown later, this

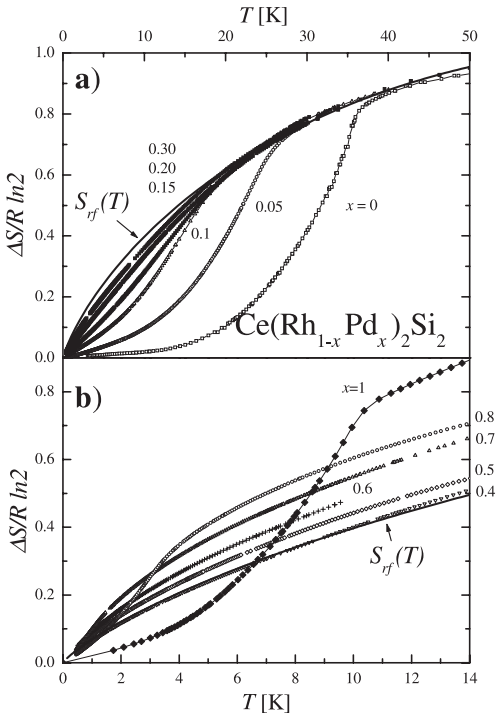


**Fig. 4.** Evolution of the temperature dependence of the magnetic entropy as a function of Pd concentration. a) Low Pd content and b) intermediate and high Pd concentration. The continuous curve ($S_{rf}$) represents the entropy related to the reference curve $C_{\rm rf}/T$ proposed in Figure 2.

curve can be described by a simple function which relates the results in the Rh-rich samples to those at intermediate and high Pd-contents. The merging to a common function means that one can define a magnetically-non-ordered state (hereafter, normal state) for all the Rh-rich samples. The temperature dependence of the (electronic/magnetic) entropy $\Delta S(T)$ of this normal state corresponds to the common function and determines the entropy observed at $T_{\rm N}(x)$ for a given composition. This is a result expected in the case where one energy scale determines $\Delta S(T)$ (and thus $C_{\rm el}(T)/T$ or $C_{\rm rf}/T$ as in Fig. 2b) of the normal state while a second independent energy scale determines the ordering temperature. This can be compared with some quasi one-dimensional spin systems, where the $C_{\rm el}(T)/T$ of the normal state is determined by the *intrachain* exchange and $T_{\rm N}$ by the *interchain* exchange, or for a superconductor (or a Spin Density Wave) where the normal state $C_{\rm el}(T)/T$ is determined by the electron density of states (*i.e.*, the band width) whereas $T_{\rm C}$ (or $T_{\rm SDW}$) is determined by the interaction between the quasiparticles. In those cases, the change of the ordering temperature $T_{\rm C}$ ($T_{\rm SDW}$) leads to a change of the entropy at $T_{\rm C}$ ($T_{\rm SDW}$) in accord with the temperature dependence of the entropy of the normal state. However, this would not be the case in a *purely* localized three-dimensional antiferromagnet where, reducing the exchange strength (and thus $T_{\rm N}$) would not change the entropy collected at $T_{\rm N}$. Therefore this result is a very strong indication that in the Rh-rich region there is a characteristic 4*f*-energy which is independent of the

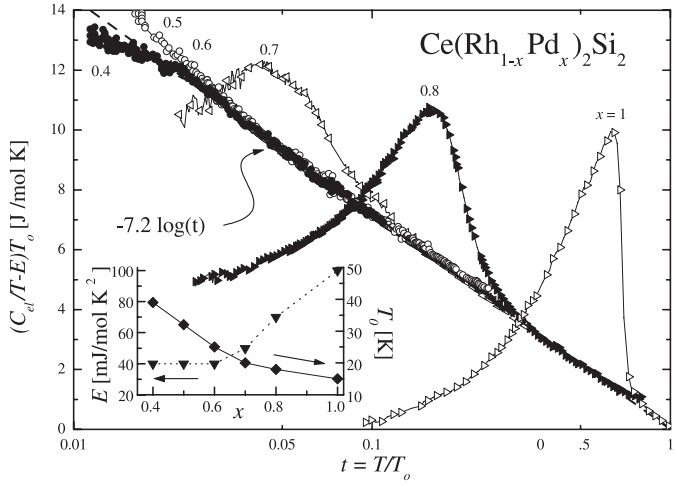


**Fig. 5.** Scaling of the specific heat as a function of a normalized temperature $t = T/T_0$. Inset: Evolution of the two fitting parameters $T_0$ and $E$ as a function of Pd doping in the $0.4 \leq x \leq 1$ range.

composition. This characteristic energy governs the normal state and it is not related to the magnetic order but to the hybridization energy of the $4f$-electrons.

In contrast to the Rh-rich region, the entropy gain in the intermediate and in the Pd-rich regions increases continuously with the Pd-content. This indicates a continuous decrease of the characteristic energy with increasing $x$ for $x \geq 0.4$. A more precise analysis can be performed by fitting the $C_{\rm el}(T)/T$ data of the samples with $0.4 \geq x \geq 1$ using a scaling formula proposed for systems close to a magnetic instability [23], $C_{\rm el}/t = -D\,\log(t) + E\,T_0$ with $t = T/T_0$, $T_0$ and $E$ being two free parameters corresponding to a characteristic energy and the linear background contribution to the specific heat, respectively. $D = 7.2\,{\rm J/mol\,K}$ is kept fixed and is related to the entropy included in the $\log(T)$ contribution, this entropy amounting to $\approx 1/2\ln 2$ at $T_0$. In reference [23], it was demonstrated that with this value of $D$, the specific heat of many Ce-based-NFL systems can be fitted giving $T_0$ values very close to those obtained in other measurements, *e.g.* neutron scattering. The fitting and the concentration dependence of $T_0$ and $E$ are shown in Figure 5. $T_0$ decreases continuously from 40 K at $x = 0.4$ to 15 K at $x = 1.0$, whereas $E$ increases continuously from 40 to $100\,{\rm mJ/mol\,K^2}$. The corresponding $\Delta S(T)$ and $C_{\rm el}(T)/T$ curves are shown as reference functions in Figure 4b (continuous line) and Figure 5 (straight line), respectively. The fitting parameters, obtained for $x = 0.4$, can be used to fit the entropy of the common normal state observed in the Rh-rich region indicating that, despite the change of regime, there is a smooth evolution of the normal state from the $x < 0.4$ to the $x > 0.4$ region. One should notice that the $T_0$ value we obtain for $CeRh_2Si_2$ and $CePd_2Si_2$ (42 K and 15 K, respectively) are close to the $T_{\rm K}$ values of 33 K and 10 K given by the inelastic neutron scattering [9]. This supports the applicability of the scaling formula. The scaling further implies that, in the absence of magnetic order (*i.e.*, in the concentration range $0.3 < x < 0.7$), $C_{\rm el}/T$ is inversely proportional to $T_0$ at very low temperatures, as in the single ion Kondo model for $T_{\rm K}$. For the samples showing magnetic order this is no longer true, since part of the degrees of freedom contributing to $C_{\rm el}/T$ condense into the magnetic state. Thus the analysis of the composition dependence of $\Delta S(T)$ and $C_{\rm el}(T)/T$ demonstrates a continuous evolution of the normal state from pure $CeRh_2Si_2$ to pure $CePd_2Si_2$. Nevertheless, a clear break in the $x$-dependence of the characteristic energy $T_0$ occurs at $x = 0.4$, since $T_0$ is constant for $x < 0.4$ but decreases continuously for $x \geq 0.4$. This change of regime underscores the different nature of the Ce ground state in both concentration limits.

As mentioned before, no discontinuity in the crystalline parameters is observed in this system [18]. The "$c/a$"-ratio, as was already mentioned, undergoes one of the largest variations observed among the Ce 122 intermetallics with $ThCr_2Si_2$ type structure [24], changing from $c/a = 2.49$ for $CeRh_2Si_2$ to 2.33 for $CePd_2Si_2$, with a weak variation in the slope at $x = 0.3$. A concomitant modification in the magnetic structure is observed between $CeRh_2Si_2$ (with the moments ordered along the $c$-axis) and $CePd_2Si_2$ (with the staggered magnetic moments on the basal plane) [21]. Such a drastic difference makes a continuity in the LRMO between both stoichiometric extremes unlikely. One would instead expect a disordered or frustrated magnetic region between those phases, but our results show that also the character of the $f$-electron localization is changing.

Further information can be obtained from a more detailed analysis of the resistivity, since its temperature dependence is dominated by the effect of the magnetic scattering. On the Rh-rich side, a clear scaling in the $\rho(T, x)$ dependence can be observed when the measured $\rho(T)$ is normalized to its value at 40 K right above $T_{\rm N}(x = 0)$ and at high temperature, *i.e.* $(\rho(T) - \rho_{40\,{\rm K}})/(\rho_{300\,{\rm K}} - \rho_{40\,{\rm K}})$, as displayed in the inset of Figure 1a. This scaling holds only for the alloys that show magnetic order (*i.e.* $x \leq 0.2$), indicating that the magnetic component involved in the electronic scattering has a different nature for the low Pd doping range than in the intermediate region. It is worth noting that the resistivity of $YCo_2$ [25], a prototype of band spin fluctuation systems, fits into this scaling, as shown in the inset of Figure 1a. This is a strong evidence for the itinerant character of the electronic properties of these alloys. Such a scaling also supports the fact that the energy which characterizes the Rh-rich region does not change with concentration. Despite its relatively large curvature, the $\rho(T)$ dependence cannot be attributed to an intermediate valence behavior (like in $CeRh_2$ for example [26]) because of LRMO at lower temperature.

The disappearance of the magnetic order is connected with a profound change in the low energy excitations. This is evidenced in the resistivity, which at low temperatures was found to follow a power law $\rho(T) = \rho_0 + a\,T^n$ with an exponent $n$ that changes systematically with composition. As an example we show in Figure 6 the temperature dependent part of the resistivity, $\Delta\rho(T) = \rho(T) - \rho_0$, in

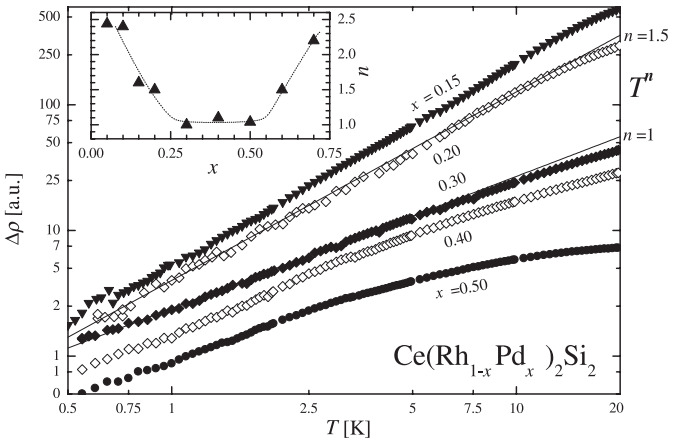


**Fig. 6.** Power law temperature dependence of the magnetic component, $\Delta\rho(T) \propto T^n$, of the electrical resistance in the low temperature region in a double logarithmic representation for the $0.15 \leq x \leq 0.5$ range. Inset: evolution of $n(x)$.

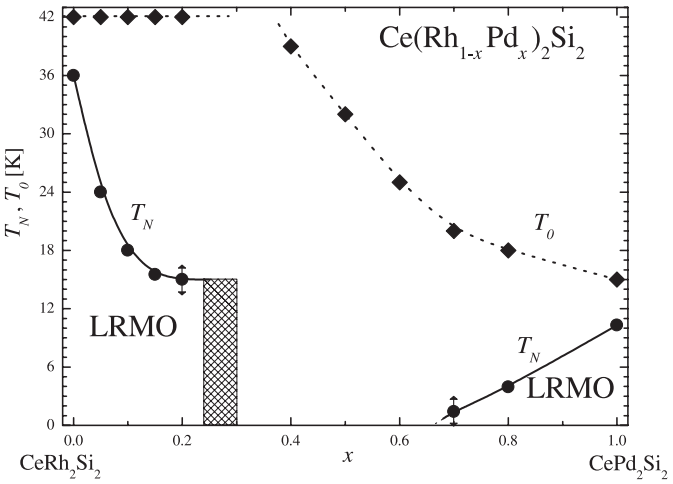


**Fig. 7.** Magnetic phase diagram as a function of Pd doping ($x$), showing the region of the magnetic ordered phases (LRMO), the transition region (shadowed area) and the evolution of the normalized scaling factor $T_0(x)$.

a log-log plot for the concentration range $0.15 \leq x \leq 0.5$. Here, the disappearance of the magnetic order leads to a strong decrease of $n$ to values close to 1, characteristic for non-Fermi Liquid systems [27]. For $x < 0.2$ and $x > 0.6$ we found values of $n$ larger than 2 as expected for compounds showing LRMO. The inset of Figure 6 shows the composition dependence of the exponent $n$.

The present investigation of the $Ce(Rh_{1-x}Pd_x)_2Si_2$ system allows us to propose a more detailed phase diagram. We have included in Figure 7 the magnetic phase boundaries, $T_N(x)$ and the evolution of the characteristic energy $T_0$ as deduced from the scaling of $C_{el}(T)/T$. The change in the evolution of $T_0$, as deduced from the $C_{el}(T)/T$ and $\rho(T)$ results, suggests the division of the magnetic phase diagram into two regions with a crossover region between $x = 0.3$ and $x = 0.4$ (hatched area). On the Rh-rich side, a strong decrease of $T_N(x)$ coexists with a constant $T_0$, while the suppression of the magnetic order occurs at a finite $T_N$ in the crossover region. On the Pd-rich side of the crossover region, $T_0$ decreases continuously with increasing $x$, with the slope becoming weaker once the magnetic order appears. The part of the phase diagram on the right (Pd-rich) side of the crossover region corresponds to that expected for a transition from a non-ordered to a magnetically ordered Kondo-lattice system. Simple models, like that proposed by Doniach, predict a monotonous decrease of $T_N$ with increasing $T_K$ in the vicinity of the transition, just as observed here for increasing Rh doping in $CePd_2Si_2$. Therefore this part of the phase diagram is in agreement with the present picture of $CePd_2Si_2$ as a localized antiferromagnet. In contrast, that part of the phase diagram on the left (Rh-rich) side of the crossover region cannot be explained within such a localized Doniach-model, since the magnetic order is suppressed without a concomitant increase of the characteristic energy. There, the scaling of the resitivity with that of $YCo_2$ and the evolution of the entropy with doping support an itinerant type of magnetic order. In itinerant systems, nesting properties are essential for the occurrence of magnetic order. Disorder, by smearing out the Fermi-surface, shall have a much stronger effect on the magnetic ordering than in localized systems, especially if the ordered state is close to the stability limit. This is certainly the case for $CeRh_2Si_2$ as shown by the strong suppression of the LRMO with pressure (one order of magnitude larger than for $CePd_2Si_2$). Then, the rapid suppression of the magnetic order upon Pd-doping despite a constant characteristic energy can easily be accounted for by the disorder due to the doping.

## 4 Conclusions

The main result of this investigation is that the Rh-rich and the Pd-rich parts of the $Ce(Rh_{1-x}Pd_x)_2Si_2$ system behave very differently. On the Pd-rich side, increasing the Rh-content leads to a pronounced increase of the characteristic $4f$-energy $T_0$ and a concomitant continuous decrease of $T_N$ down to 0 K. This side of the magnetic phase diagram corresponds to the predictions of models based on localized $f$-electrons, supporting the current interpretation of a localized antiferromagnetic state in $CePd_2Si_2$. In contrast, on the Rh-rich side, Pd doping leads to a continuous decrease of the degrees of freedom involved in the magnetic ordered state and to the disappearance of the magnetic state at a finite $T_N$, despite the fact that the characteristic energy $T_0$ is not affected by the Pd-doping. This points to an itinerant type of magnetic order in $CeRh_2Si_2$, which is destroyed by the disorder introduced by the Pd-doping. Further evidence for the itinerant character is that $\rho(T)$ in the Rh-rich region scales with that of $YCo_2$, a prototype band spin-fluctuation system. The change of slope in the dependence of $T_0$ on composition between $x = 0.3$ and $x = 0.4$ suggests that the change from the itinerant to the localized regimes takes place in that region. In the intermediate region $0.4 < x < 0.6$, we observe in $\rho(T < 5\,\mathrm{K})$

a power law with an exponent $n$ close to 1, which we attribute to the disorder induced by the alloying and to the absence of long range magnetic order.

This work was partially supported by joint programs between Fundación Antorchas (Arg.) and Alexander von Humboldt Stiftung (Germ.) #A-13391/1-003, Fundación Antorchas and DAAD (Germ.) #13740/1-88 and ANPCyT: project PICT #03-3250. MGB, PP and JGS, are members of the Consejo Nacional de Investigaciones Científicas y Técnicas (Arg.).

## References

1. C. Godard, L.C. Gupta, M.F. Ravet-Krill, J. Less Comm. Met. **94**, 187 (1983)
2. A. Szytula, A. Budkowski, M. Slaski, R. Zach, Solid State Commun. **57**, 813 (1986)
3. S. Quezel, J. Rossat-Mignot, B. Chevalier, P. Lejay, J. Etorneau, Solid State Commun. **49**, 685 (1984)
4. T. Graf, M.F. Hundley, R. Modler, R. Movshovich, J.D. Thompson, D. Mandrus, R.A. Fisher, N.E. Phillips, Phys. Rev. B **57**, 7442 (1998)
5. R. Settai, A. Misawa, S. Araki, M. Koski, K. Sigiyama, T. Takeuchi, K. Kindo, Y. Haga, E. Yamamamoto, Y. Önuki, J. Phys. Soc. Jpn **66**, 2260 (1997)
6. D. Gignoux, D. Schmitt, *Handbook of Magnetic Materials*, Vol. 10, Chap. 2, edited by K.H.J. Buschow (Elsevier Science, B.V., 1997), pp. 239–414
7. S. Araki, R. Settai, T.C. Kabayashi, Y. Önuki, Phys. Rev. B **64**, 224417 (2001)
8. S. Araki, A. Misawa, R. Settai, T. Takeuchi, Y. Önuki, J. Phys. Soc. Jpn **67**, 2915 (1998)
9. A. Severing, E. Holland-Moritz, B. Frick, Phys. Rev. B **39**, 4164 (1989)
10. Y. Kawasaki, K. Ishida, Y. Kitaoka, K. Asayama, Phys. Rev. B **58**, 8634 (1998)
11. S. Kawarazaki, M. Sato, Y. Miyako, N. Chigusa, K. Watanabe, N. Metoki, Y. Koibe, M. Nishi, Phys. Rev. B **61**, 4167 (1999)
12. J.D. Thompson, R.D. Parks, H. Borges, J. Magn. Magn. Matter. **54-57**, 377 (1986)
13. S. Doniach, Physica B **91**, 231 (1977)
14. T. Endstra, G.J. Nieuwenhuys, J.A. Mydosh, Phys. Rev. B **48**, 9595 (1993)
15. C. Godart, L.C. Gupta, C.V. Tomy, J.D. Thompson, R. Vijayaraghavan, Europhys. Lett. **8**, 375 (1989)
16. J.D. Thompson, H. Hegger, D. Louca, G.H. Kwei, R. Movshovich, C. Petrovic, J.L. Serrao, J. Alloys Comp. **303-304**, 239 (2000)
17. N.D. Mathur, F.M. Grosche, S.R. Julian, I.R. Walker, D.M. Freye, R.K.W. Haselwimmer, G.G. Lonzarich, Nature **394**, 39 (1998)
18. O. Trovarelli, M. Gómez Berisso, P. Pedrazzini, D. Bosse, C. Geibel, J.G. Sereni, F. Steglich, J. Alloys Comp. **275-277**, 569 (1998)
19. M. Gómez Berisso, P. Pedrazzini, J.G. Sereni, O. Trovarelli, C. Geibel, F. Steglich, Physica B **259-261**, 68 (1999)
20. D. Cornut, B. Coqblin, Phys. Rev. B **5**, 4541 (1972)
21. B.H. Grier, J.M. Lawrence, V. Murgai, R.D. Parks, Phys. Rev. B **29**, 2664 (1984)
22. T. Moriya, T. Takimoto, J. Phys. Soc. Jpn **64**, 960 (1995)
23. J.G. Sereni, C. Geibel, M. Gómez Berisso, P. Hellmann, O. Trovarelli, F. Steglich, Physica B **230-232**, 580 (1997)
24. G. Just, P. Paufler, J. Alloys Comp. **232**, 1 (1996)
25. R. Hauser, E. Bauer, E. Gratz, Phys. Rev. B **57**, 2904 (1998)
26. A. Harrus, T. Mihalisin, E. Kemly, J. Magn. Magn. Matter. **47&48**, 93 (1985)
27. H.v. Löhneysen, J. Phys. Cond. Matt. **8**, 9689 (1996)